



Cite this: *CrystEngComm*, 2014, 16, 11088

The various architectures and properties of a series of coordination polymers tuned by the central metals and auxiliary N-donor ligands†

He Wu,^a Wujuan Sun,^a Ting Shi,^a Xuzhao Liao,^a Wenjie Zhao^b and Xuwu Yang^{*a}

Five new coordination polymers, namely, $[\text{Zn}(\text{HL})(\text{bib})]_n \cdot 2n\text{H}_2\text{O}$ (**1**), $[\text{Zn}_2(\text{L})(\mu_3\text{-OH})(\text{H}_2\text{O})]_n \cdot 2n\text{H}_2\text{O}$ (**2**), $[\text{Cd}_{1.5}(\text{L})(\text{H}_2\text{O})_2]_n \cdot 0.5n\text{H}_2\text{O}$ (**3**), $[\text{Cd}_{1.5}(\text{L})(\text{CH}_3\text{CN})]_n \cdot 0.5n\text{H}_2\text{O}$ (**4**) and $[\text{Cd}_{1.5}(\text{L})(\text{bib})(\text{H}_2\text{O})_2]_n \cdot n\text{H}_2\text{O}$ (**5**), (H_3L = biphenyl-2,4',5-tricarboxylic acid, bib = 4,4'-bis(imidazol-1-yl)phenyl) have been synthesized under solvothermal conditions. Complexes **1–5** have been characterized by elemental analysis, IR spectroscopy, powder X-ray diffraction (PXRD) and single-crystal X-ray diffraction analysis. Complex **1** shows a 2D (4,4) network and further forms a 3D supramolecular framework by π - π interactions. Complex **2** is a 3D framework based on infinite rod-shaped chains. Complex **3** exhibits a 3D framework with a (3,4,5)-connected $\{4^2 \cdot 6\}_2\{4^2 \cdot 8^4\}\{4^3 \cdot 6 \cdot 8^6\}_2$ topology. Complex **4** features a 3D network with a (4,4,6)-connected $\{4^4 \cdot 6^2\}_3\{4^6 \cdot 6^7 \cdot 8^2\}_2$ topology. **5** displays a 3D 2-fold interpenetrating (4,4,4)-connected framework with a point symbol of $\{4 \cdot 6^4 \cdot 10\}_2\{4 \cdot 6^4 \cdot 8\}_2\{6^2 \cdot 8^4\}$. Moreover, the thermal stabilities and photoluminescence properties of **1–5** have been investigated.

Received 2nd August 2014,
Accepted 14th October 2014

DOI: 10.1039/c4ce01602e

www.rsc.org/crystengcomm

Introduction

The design and construction of coordination polymers have received great attention because of their intriguing topology¹ as well as potential applications in the areas of photoluminescence,² ion exchange,³ gas and hydrocarbon separation and storage,⁴ catalysis,⁵ and magnetism.⁶ Until now, the rational design and synthesis of coordination polymers with expected structures are still challenges for researchers. It is well known that the construction of coordination polymers is mainly dependent on several factors, such as central metals,⁷ inorganic/organic anions,⁸ N-donor ligands,⁹ pH values,¹⁰ reaction temperatures,¹¹ etc. Among these, the organic anions play crucial roles in the construction of coordination polymers.¹²

In this regard, the aromatic multicarboxylate ligands have been proven to be excellent candidates for building highly connected, self-penetrating or helical coordination

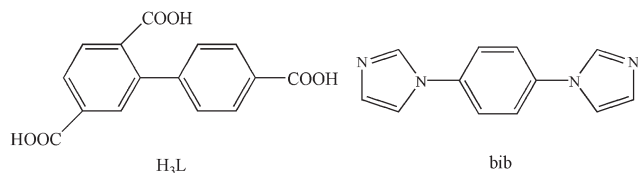
frameworks due to their versatile bridging fashions.¹³ Up to now, aromatic multicarboxylate ligands, such as 1,4-benzenedicarboxylic acid,¹⁴ 1,3,5-benzenetricarboxylic acid¹⁵ and 1,2,4,5-benzenetetracarboxylic acid,¹⁶ have been extensively utilized in the construction of coordination polymers. Compared to the above rigid multicarboxylate ligands, biphenyltricarboxylic acid is a flexible and longer ligand. The biphenyltricarboxylic acid ligand has three carboxylic groups that may be completely or partially deprotonated, inducing various coordination modes and allowing interesting structures with higher dimensionality. In addition, this ligand can conform to the coordination geometries of the metal ions because its two phenyl rings can be rotated around the C–C single bond.¹⁷ Until now, various biphenyltricarboxylic acid ligands, such as biphenyl-3,3',5-tricarboxylic acid¹⁸ and biphenyl-3,4',5-tricarboxylic acid,¹⁹ have been widely used to construct coordination polymers. However, to the best of our knowledge, there are no coordination polymers based on biphenyl-2,4',5-tricarboxylic acid reported to date. Thus, it is necessary to construct new coordination polymers based on biphenyl-2,4',5-tricarboxylic acid and investigate their properties.

Herein, for the first time, we report the synthesis and characterization of five coordination polymers based on biphenyl-2,4',5-tricarboxylic acid and N-donor ligands (Scheme 1) under solvothermal conditions, namely, $[\text{Zn}(\text{HL})(\text{bib})]_n \cdot 2n\text{H}_2\text{O}$ (**1**), $[\text{Zn}_2(\text{L})(\mu_3\text{-OH})(\text{H}_2\text{O})]_n \cdot 2n\text{H}_2\text{O}$ (**2**), $[\text{Cd}_{1.5}(\text{L})(\text{H}_2\text{O})_2]_n \cdot 0.5n\text{H}_2\text{O}$ (**3**), $[\text{Cd}_{1.5}(\text{L})(\text{CH}_3\text{CN})]_n \cdot 0.5n\text{H}_2\text{O}$ (**4**), and

^a Key Laboratory of Synthetic and Natural Functional Molecule Chemistry of Ministry of Education, Shaanxi Key Laboratory of Physico-Inorganic Chemistry, College of Chemistry & Materials Science, Northwest University, Xi'an 710069, PR China. E-mail: yangxuwu@nwnu.edu.cn; Tel: +86 29 88302054

^b Department of Biochemical Engineering, Xianyang Vocational Technical college, Xianyang, 712000, PR China

† Electronic supplementary information (ESI) available: Selected bond lengths and angles, TGA curves, PXRD. CCDC 1012794–1012798. For ESI and crystallographic data in CIF or other electronic format see DOI: 10.1039/c4ce01602e



Scheme 1 Structure of H₃L and bib ligands.

[Cd_{1.5}(L)(bib)(H₂O)₂]_n·*n*H₂O (5). These complexes exhibit a systematic variation of architectures from the 2D layer to 3D frameworks. In addition, the photoluminescence properties of 1–5 in the solid state have also been investigated.

Experimental section

Materials and general methods

The ligands H₃L and bib were purchased from Jinan Camolai Trading Company; the other starting reagents and solvents employed were purchased commercially and used directly without further purification. The powder X-ray diffraction patterns were collected on a Bruker D8 ADVANCE X-ray powder diffractometer (Cu Kα, λ = 1.5418 Å). The FT-IR spectra were measured in the range of 4000–400 cm^{−1} on a Bruker EQUINOX-55 spectrometer with KBr pellets. Elemental analyses of C, H and N were performed on a PerkinElmer 2400C elemental analyzer. The solid-state emission/excitation spectra were recorded with a Hitachi F-4500 fluorescence spectrophotometer at room temperature. Thermogravimetric analyses (TGA) were carried out under nitrogen stream using a NETZSCH STA449C instrument with a heating rate of 10 °C min^{−1}.

Synthesis of [Zn(HL)(bib)]_n·2*n*H₂O (1). A mixture of ZnCl₂ (5.44 mg, 0.04 mmol), H₃L (5.72 mg, 0.02 mmol) and bib (4.20 mg, 0.02 mmol) was dissolved in 6 mL of CH₃CN/H₂O (3 : 1, v/v). The final mixture was placed in a Teflon-lined stainless steel container, heated at 130 °C for 72 h and then cooled to room temperature at a rate of 5 °C h^{−1}. Colorless crystals were obtained (yield: 56% based on H₃L). Anal. calcd for C₂₇H₂₂ZnN₄O₈: C, 54.42; H, 3.72; N, 9.40%. Found: C, 54.38; H, 3.75; N, 9.43%. IR (KBr, cm^{−1}): 3426(m), 3130(m), 2540(w), 2027(w), 1712(m), 1591(s), 1533(s), 1492(w), 1404(s), 1369(m), 1312(m), 1187(w), 1068(m), 956(w), 838(m), 773(m), 705(w), 652(m), 581(w), 543(w), 500(w).

Synthesis of [Zn₂(L)(μ₃-OH)(H₂O)]_n·2*n*H₂O (2). A mixture of Zn(OAc)₂·2H₂O (6.58 mg, 0.03 mmol), H₃L (5.72 mg, 0.02 mmol) and H₂O (3 mL) was placed in a Teflon-lined stainless steel container, heated at 130 °C for 72 h and then cooled to room temperature at a rate of 5 °C h^{−1}. Colorless crystals were obtained (yield: 49% based on H₃L). Anal. calcd for C₁₅H₁₄Zn₂O₁₀: C, 37.14; H, 2.91%. Found: C, 37.20; H, 2.83%. IR (KBr, cm^{−1}): 3425(m), 2027(w), 1593(m), 1542(s), 1410(s), 1295(w), 1186(w), 1103(w), 1017(w), 871(m), 773(m), 707(w), 610(w), 574(w), 500(w).

Synthesis of [Cd_{1.5}(L)(H₂O)₂]_n·0.5*n*H₂O (3). A mixture of 3CdSO₄·8H₂O (23.08 mg, 0.03 mmol) and H₃L (5.72 mg, 0.02 mmol) was dissolved in 4.5 mL of DMF/CH₃OH/H₂O

(1 : 4 : 4, v/v/v). The final mixture was placed in a Teflon-lined stainless steel container, heated at 150 °C for 36 h and then cooled to room temperature over a period of 48 h. Colorless crystals were obtained (yield: 62% based on H₃L). Anal. calcd for C₁₅H₁₂Cd_{1.5}O_{8.5}: C, 35.26; H, 2.43%. Found: C, 35.34; H, 2.50%. IR (KBr, cm^{−1}): 3428(m), 2027(w), 1579(m), 1539(m), 1403(s), 1294(w), 1185(w), 1106(w), 1015(w), 854(m), 775(s), 709(m), 580(m), 518(w), 466(m).

Synthesis of [Cd_{1.5}(L)(CH₃CN)]_n·0.5*n*H₂O (4). A mixture of Cd(NO₃)₂·4H₂O (13.88 mg, 0.045 mmol) and H₃L (5.72 mg, 0.02 mmol) was dissolved in 4.5 mL of CH₃CN/H₂O (1 : 2, v/v). The final mixture was placed in a Teflon-lined stainless steel container, heated at 150 °C for 36 h and then cooled to room temperature over a period of 48 h. Colorless crystals were obtained (yield: 54% based on H₃L). Anal. calcd for C₁₇H₁₁Cd_{1.5}NO_{6.5}: C, 40.68; H, 2.21; N, 2.79%. Found: C, 40.65; H, 2.24; N, 2.77%. IR (KBr, cm^{−1}): 3602(m), 3395(w), 2925(w), 2545(w), 2362(w), 2296(w), 2270(m), 2028(w), 1849(w), 1566(s), 1500(m), 1403(s), 1259(w), 1140(w), 1038(w), 925(w), 865(m), 827(m), 767(s), 710(m), 656(s), 610(s), 559(m), 515(m), 471(m).

Synthesis of [Cd_{1.5}(L)(bib)(H₂O)₂]_n·*n*H₂O (5). A mixture of Cd(NO₃)₂·4H₂O (6.16 mg, 0.02 mmol), H₃L (5.72 mg, 0.02 mmol) and bib (4.20 mg, 0.02 mmol) was dissolved in 6 mL of DMF/H₂O (1 : 5, v/v). The final mixture was placed in a Teflon-lined stainless steel container, heated at 130 °C for 72 h and then cooled to room temperature at a rate of 5 °C h^{−1}. Colorless crystals were obtained (yield: 58% based on H₃L). Anal. calcd for C₂₇H₂₃Cd_{1.5}N₄O₉: C, 45.28; H, 3.24; N, 7.82%. Found: C, 45.25; H, 3.28; N, 7.79%. IR (KBr, cm^{−1}): 3482(w), 2427(w), 2027(m), 1622(m), 1528(w), 1399(m), 1068(s), 1011(s), 754(w), 670(w), 582(m), 525(m).

X-ray crystallographic studies

Intensity data were collected on a Bruker Smart APEX II CCD diffractometer with graphite-monochromated Mo Kα radiation (λ = 0.71073 Å) at room temperature. The structure was solved by direct methods and refined with full-matrix least-squares on *F*² with the SHELXL-97 program package and OLEX-2 suite. An empirical absorption correction was applied using the SADABS program. During refinement of 1 and 5, two lattice water molecules were split over two sites. During refinement of 2, one lattice water molecule was found to be disordered, so squeeze refinement was performed. The contributions of all the solvent atoms have been incorporated in both the empirical formulas and formula weights. The hydrogen atoms which are attached to the disordered O atoms of 3 could not be positioned geometrically. Crystal data and refinement parameters of 1–5 are shown in Table 1, and the selected bond lengths and angles are listed in Table S1.†

Results and discussion

X-ray crystallographic studies reveal that complex 1 is a monoclinic crystal system with *P*2(1)/*n* space group. The asymmetric unit contains one Zn(II) ion, one HL^{2−} ligand,

Table 1 Crystal and structure refinement data for 1–5

Complex	1	2	3	4	5
Formula	C ₂₇ H ₂₂ ZnN ₄ O ₈	C ₁₅ H ₁₄ Zn ₂ O ₁₀	C ₁₅ H ₁₂ Cd _{1.5} O _{8.5}	C ₁₇ H ₁₁ Cd _{1.5} NO _{6.5}	C ₂₇ H ₂₃ Cd _{1.5} N ₄ O ₉
Fw	595.86	485.00	496.87	501.89	716.11
T (K)	296(2)	296(2)	296(2)	296(2)	296(2)
Crystal system	Monoclinic	Orthorhombic	Monoclinic	Monoclinic	Monoclinic
Space group	<i>P</i> 2(1)/ <i>n</i>	<i>Pbca</i>	<i>C</i> 2/ <i>c</i>	<i>C</i> 2/ <i>c</i>	<i>P</i> 2/ <i>n</i>
<i>a</i> (Å)	7.8024(13)	20.2193(4)	29.778(2)	10.0131(12)	10.0418(12)
<i>b</i> (Å)	15.776(3)	6.5716(1)	6.6754(5)	24.639(3)	9.7038(12)
<i>c</i> (Å)	22.417(4)	27.935(5)	19.4782(14)	13.7618(16)	26.051(3)
α (deg)	90.00	90.00	90.00	90.00	90.00
β (deg)	100.022(3)	90.00	113.6230(10)	109.151(2)	95.109(2)
γ (deg)	90.00	90.00	90.00	90.00	90.00
<i>V</i> (Å ³)	2717.2(8)	3711.8(6)	3547.4(4)	3207.3(7)	2528.4(5)
<i>Z</i>	4	8	4	4	2
<i>D_c</i> (g cm ^{−3})	1.457	1.671	1.859	2.079	1.881
<i>F</i> (000)	1224	1872	1932	1944	1428
μ (mm ^{−1})	0.960	2.628	1.855	2.046	1.339
Reflns collected	10 949	17 375	9277	9105	13 572
Reflns unique	4552	3270	3603	3457	5084
<i>R</i> _{int}	0.0689	0.0805	0.0269	0.0669	0.0771
GOF	1.013	1.010	1.055	1.003	1.015
<i>R</i> ₁ , <i>a R</i> ₂ ^b [<i>I</i> > 2σ(<i>I</i>)]	0.0617, 0.1639	0.0401, 0.0972	0.0370, 0.1361	0.0488, 0.1064	0.0574, 0.1065
<i>R</i> ₁ , w <i>R</i> ₂ (all data)	0.1071, 0.1878	0.0647, 0.1197	0.0507, 0.1484	0.0890, 0.1372	0.0893, 0.1284

$$^a R_1 = \sum ||F_o| - |F_c|| / \sum |F_o|, \quad ^b wR_2 = \sum [w(F_o^2 - F_c^2)^2] / \sum [w(F_o^2)^2]^{1/2}.$$

one bib ligand and two lattice water molecules. The Zn(II) ion is five coordinated with two nitrogen atoms from two bib ligands and three carboxylic oxygen atoms from two HL^{2−} ligands, forming a distorted square-pyramidal coordination geometry (Fig. 1a). The Zn–O and Zn–N bonds are in the range of 1.950(5)–2.213(7) and 2.009(6)–2.012(5) Å, respectively. In 1, each adjoining pair of Zn(II) ions is

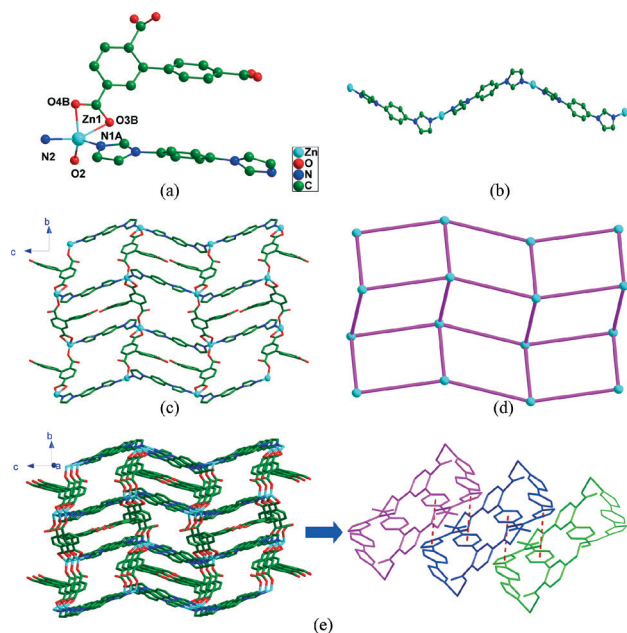
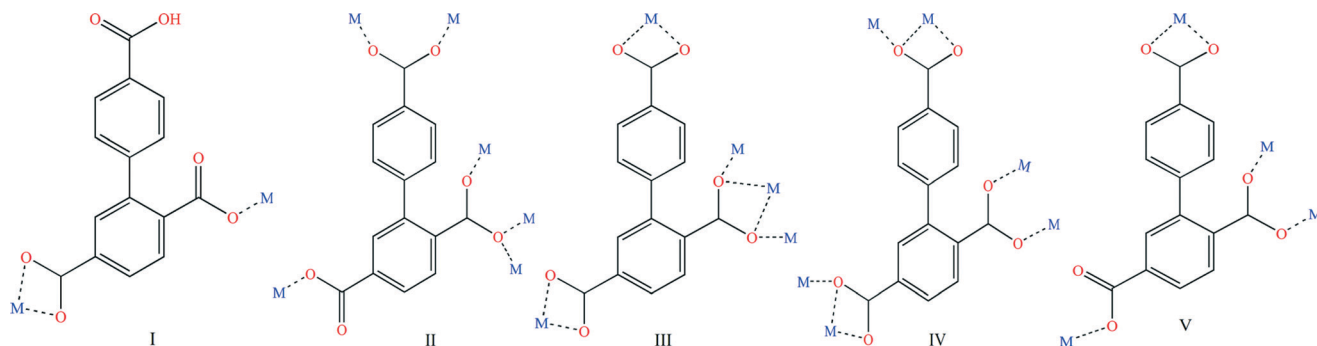


Fig. 1 (a) Coordination environment of Zn(II) ion in complex 1. (b) View of the 1D chain in complex 1. (c) View of the 2D network in complex 1. (d) View of the topology framework of complex 1. (e) 3D supramolecular architecture of 1 formed by π – π stacking. Symmetry codes: (A) $x + 1/2, -y + 3/2, z - 1/2$; (B) $-x + 3/2, y - 1/2, -z + 1/2$.

connected by bib ligands to form a [Zn(bib)]_n chain (Fig. 1b). The adjacent [Zn(bib)]_n chains are linked by HL^{2−} to give rise to a stair-shaped network of [Zn(HL)(bib)]_n extending in the *bc* plane (Fig. 1c). The carboxylate groups ligate to the metal ions in a μ_2 - η^0 : η^1 : η^1 : η^0 : η^0 coordination mode (mode I, Scheme 2). If the Zn(II) center is simplified to a 4-connected node, the HL^{2−} and bib ligands act as 2-connected linkers; the overall topology can be described as a 2D (4,4) network, and the topology is shown in Fig. 1d. Finally, the 3D supermolecular framework is obtained by π – π stacking interactions (Fig. 1e). The effective free volume of the channels is estimated to be 446.9 Å³ using the PLATON software, almost 16.4% of the per unit cell volume 2717.2(8) Å³; the yellow sphere represents the large pores defined within the framework (Fig. 2).

Crystal structure of [Zn₂(L)(μ_3 -OH)(H₂O)]_n·2nH₂O (2)

Complex 2 crystallizes in the orthorhombic system with *Pbca* space group, possessing a 3D structure. The asymmetric unit contains two crystallographically unique Zn(II) ions, one L^{3−} ligand, one μ_3 -OH ion, one coordinated and two lattice water molecules. As shown in Fig. 3a, there are two Zn(II) centers with different coordination environments in the asymmetric unit. The Zn1 center exhibits a distorted square-pyramidal geometry and is five coordinated by four oxygen atoms from four different L^{3−} ligands and one oxygen atom from one μ_3 -OH ion. Comparably, the Zn2 center is five coordinated by two carboxylate oxygen atoms from two different L^{3−} ligands, two μ_3 -OH oxygen atoms and one oxygen atom from one coordinated water molecule. The Zn–O bond is in the range of 1.932(4)–2.096(4) Å. The wholly deprotonated carboxylate groups of the L^{3−} ligand adopt a



Scheme 2 Coordination modes of H_3L in complexes 1–5.

$\mu_6\text{-}\eta_1:\eta_2:\eta_0:\eta_1:\eta_1:\eta_1$ coordination mode (mode II, Scheme 2). It should be noted that the OH^- ion, adopting a μ_3 -bridging coordination mode, takes part in the construction of the framework. Two $Zn(II)$ centers ($Zn1$ and $Zn2$) are bridged by two carboxylate groups to generate dinuclear SBUs ($Zn\cdots Zn = 3.1108(13)$ Å), such adjacent dinuclear SBUs are connected alternatively through the carboxylate groups of L^{3-} and $\mu_3\text{-}OH^-$ ion, forming a 1D infinite rod-shaped chain (Fig. 3b, c). In 2, the infinite rod-shaped chains are further extended by L^{3-} to form a 3D framework (Fig. 3d). Viewed along the b axis, the 1D oval channel is shown in the 3D framework, which is occupied by water molecules. The effective free volume of the channels is estimated to be 1005.6 Å³ using the PLATON software, almost 27.1% of the per unit cell volume 3711.8 Å³; the yellow sphere represents the large pores defined within the framework (Fig. 3e).

Crystal structure of $[Cd_{1.5}(L)(H_2O)_2]_n \cdot 0.5nH_2O$ (3)

Complex 3 crystallizes in the monoclinic system with $C2/c$ space group. The asymmetric unit of 3 contains one and a half independent $Cd(II)$ ions, one L^{3-} ligand, two coordinated and half a lattice water molecule. As shown in Fig. 4a, $Cd1$ lies on a crystallographic 2-fold axis and is coordinated to eight oxygen atoms from four L^{3-} ligands to form a distorted cubic geometry with $Cd1\text{--}O$ distances of $2.393(4)$ – $2.494(4)$ Å. $Cd2$ is six-coordinated by two water molecules and four carboxylic oxygen atoms from three

different L^{3-} ligands, adopting a distorted octahedral geometry with $Cd2\text{--}O$ distances of $2.233(5)$ – $2.494(4)$ Å. The wholly deprotonated carboxylate groups of the L^{3-} ligand adopt a $\mu_5\text{-}\eta_2:\eta_2:\eta_1:\eta_1:\eta_1:\eta_1$ coordination mode (mode III, Scheme 2). In 3, four $Cd(II)$ ions and four oxygen atoms from four L^{3-} ligands form a 8-membered macrocyclic ring, which is further extended by $Cd1$ and carboxylate groups to give a 1D infinite chain (Fig. 4b, c). And then, the ligand L^{3-} connects the 1D metal carboxylate chains, extending forward or backward, to generate a 3D framework structure (Fig. 4d). From a topological point of view, the $Cd1$ center acts as a 4-connected node, the $Cd2$ center acts as a 3-connected node, the L^{3-} ligand acts as a 5-connected node and the structure of 3 can be represented as a $(3,4,5)$ -connected net with a point symbol of $\{4^2 \cdot 6\}_2\{4^2 \cdot 8^4\}\{4^3 \cdot 6 \cdot 8^6\}_2$ (Fig. 4e). The effective free volume of the channels is estimated to be 682.1 Å³ using the PLATON software, almost 19.2% of the per unit cell volume 3547.4 Å³; the yellow sphere represents the large pores defined within the framework (Fig. 5).

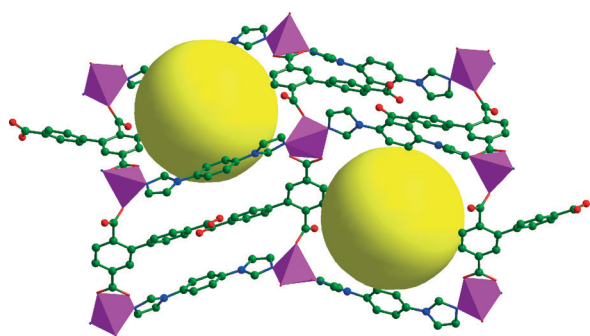


Fig. 2 Schematic representation of the large pores in the framework of 1.

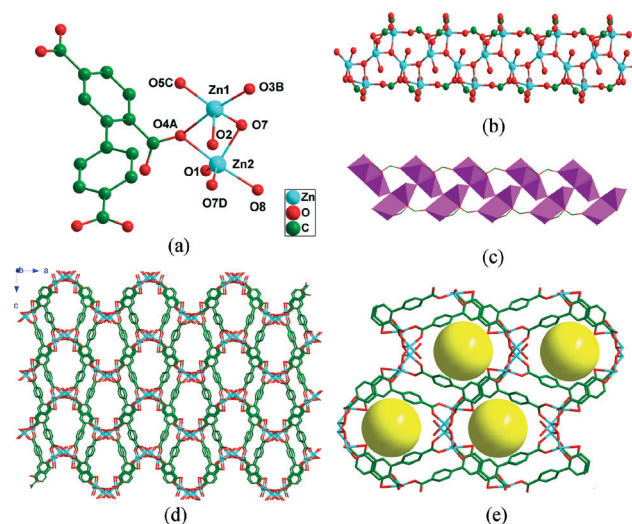


Fig. 3 (a) Coordination environment of $Zn(II)$ ions in complex 2. (b) Ball-and-stick representation of the infinite rod-shaped chain. (c) Chain with Zn shown as polyhedra. (d) Schematic representation of the 3D framework of 2. (e) Schematic representation of the large pores in the framework of 2. Symmetry codes: (A) $-x, y + 1/2, -z + 3/2$; (B) $-x, y - 1/2, -z + 3/2$; (C) $x, -y + 3/2, z - 1/2$; (D) $-x + 1/2, y + 1/2, z$.

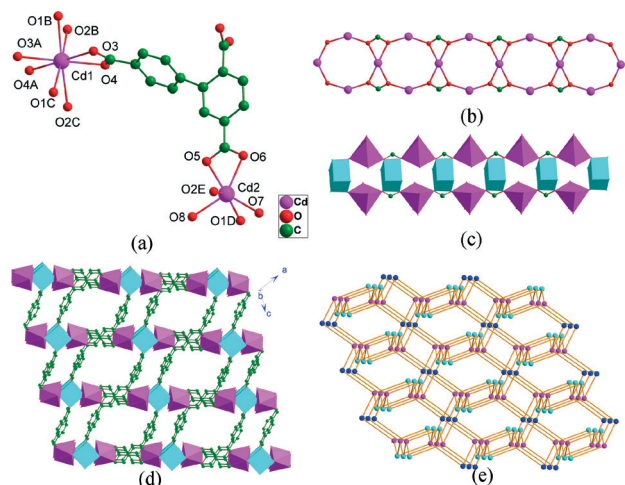


Fig. 4 (a) Coordination environment of Cd(II) ions in complex **3**. (b) Ball-and-stick representation of the infinite rod-shaped chain. (c) Chain with Cd shown as polyhedra. (d) Schematic representation of the 3D framework of **3**. (e) View of the topological net of **3** (the blue ones for Cd1 centers, the aqua ones for Cd2 centers and the pink ones for L^{3-} ligands). Symmetry codes: (A) $-x + 1, y, -z + 1/2$; (B) $-x + 1, -y + 2, -z + 1$; (C) $x, -y + 2, z - 1/2$; (D) $-x + 1/2, -y + 3/2, -z + 1$; (E) $-x + 1/2, -y + 5/2, -z + 1$.

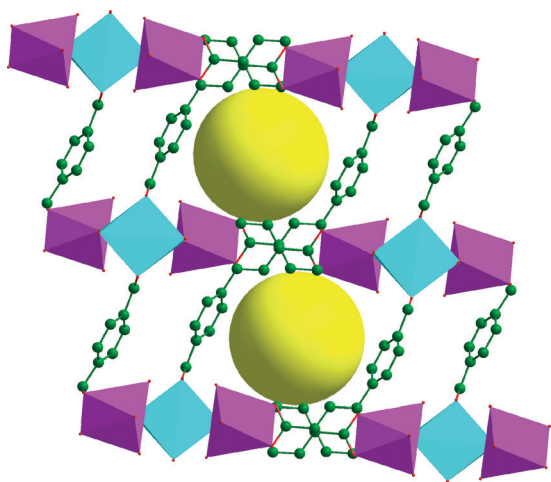


Fig. 5 Schematic representation of the large pores in the framework of **3**.

Crystal structure of $[Cd_{1.5}(L)(CH_3CN)]_n \cdot 0.5nH_2O$ (**4**)

Complex **4** crystallizes in the monoclinic system with $C2/c$ space group. The asymmetric unit of **4** contains one and a half independent Cd(II) ions, one L^{3-} ligand, one coordinated acetonitrile molecule and half a lattice water molecule. As depicted in Fig. 6a, Cd1 is coordinated to two nitrogen atoms from two acetonitrile molecules and four carboxylate oxygen atoms from four L^{3-} ligands, while Cd2 is coordinated to six carboxylate oxygen atoms from four L^{3-} ligands. The Cd–O bond lengths are in the range of 2.158(5)–2.539(5) Å, and the Cd–N one is 2.305(8) Å. Interestingly, the Cd1 ion lies on the crystallographic 2-fold axis. In addition, the O7 atom in the water molecule also lies on the 2-fold axis. The wholly

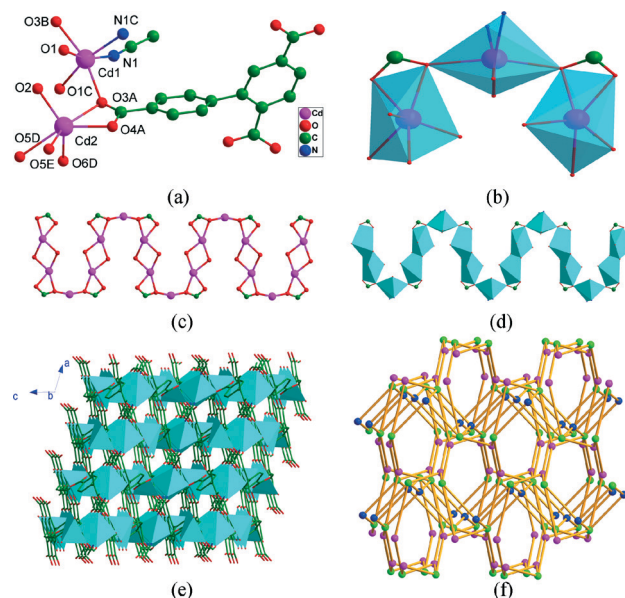


Fig. 6 (a) Coordination environment of Cd(II) ions in complex **4**. (b) The octahedral secondary building units. (c) Ball-and-stick representation of the infinite rod-shaped chain. (d) Chain with Cd shown as polyhedra. (e) Schematic representation of the 3D framework of **4**. (f) View of the topological net of **4** (the blue ones for Cd1 centers, the pink ones for Cd2 centers and the green ones for L^{3-} ligands). Symmetry codes: (A) $x + 1/2, -y + 3/2, z + 1/2$; (B) $-x + 3/2, -y + 3/2, -z + 1$; (C) $-x + 2, y, -z + 3/2$; (D) $x + 1, -y + 1, z + 1/2$; (E) $-x + 1, y, -z + 3/2$.

deprotonated carboxylate groups of the L^{3-} ligand adopt a $\mu_6\text{-}\eta_1\eta_1\eta_1\eta_2\eta_2\eta_1$ coordination mode (mode IV, Scheme 2). The L^{3-} ligands connect Cd1 and Cd2 to form the $[Cd_3(COO)_2]$ secondary building units (SBUs) (Fig. 6b), such adjacent SBUs are connected alternatively through the carboxylates of L^{3-} , forming a linear metal carboxylate chain (Fig. 6c, d). The 1D chains are further connected together by L^{3-} ligands, resulting in a 3D structure (Fig. 6e), in which each L^{3-} ligand connects six Cd(II) cations, and each Cd(II) cation links four L^{3-} ligands. Consequently, a rare (4,4,6)-connected 3D topological network with a point symbol of $\{4^4 \cdot 6^2\}_3\{4^6 \cdot 6^7 \cdot 8^2\}_2$ is generated (Fig. 6f).

Crystal structure of $[Cd_{1.5}(L)(bib)(H_2O)_2]_n \cdot nH_2O$ (**5**)

Complex **5** crystallizes in the monoclinic system with $P2_1/n$ space group. The asymmetric unit consists of one and a half independent Cd(II) ions, one L^{3-} ligand, one bib ligand, two coordinated water molecules and one lattice water molecule. As depicted in Fig. 7a, Cd1 lies on a crystallographic 2-fold axis and is coordinated to six oxygen atoms to form a distorted CdO_6 octahedral geometry [Cd–O = 2.256(5)–2.434(6) Å]. Cd2 is octahedrally coordinated by four oxygen atoms from two L^{3-} ligands, two water molecules and two nitrogen atoms from two bib ligands, [Cd–O = 2.283(5)–2.436(5) Å, Cd–N = 2.288(6)–2.305(6) Å]. In **5**, each adjoining pair of Cd2 ions is connected by bib ligands to form a $[Cd(bib)]_n$ chain. As shown in Fig. 7b, the one-dimensional chains are parallel to each other and bridged with L^{3-} ligands, thus

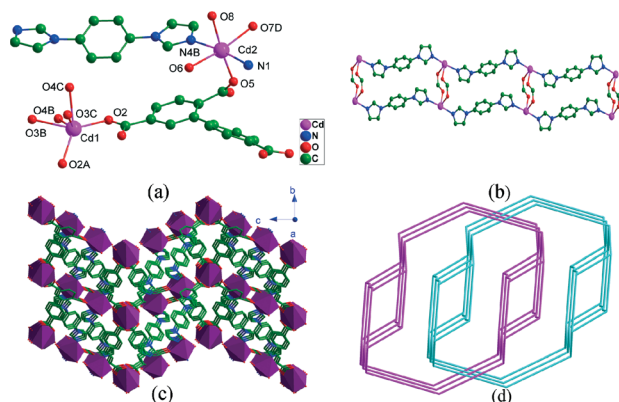


Fig. 7 (a) Coordination environment of Cd(II) ions in complex 5. (b) View of the one-dimensional double chain. (c) Schematic representation of the 3D framework of 5. (d) Schematic representation of the 3D 2-fold interpenetrating framework of 5. Symmetry codes: (A) $-x + 1/2, y, -z + 1/2$; (B) $x - 1, y - 1, z$; (C) $-x + 3/2, y - 1, -z + 1/2$; (D) $-x + 2, -y + 1, -z + 1$.

forming a one-dimensional double chain. The 1D chains are connected *via* L^{3-} ligands with a $\mu_4\text{-}\eta_1\text{:}\eta_1\text{:}\eta_1\text{:}\eta_0\text{:}\eta_1\text{:}\eta_1$ coordination mode (mode V, Scheme 2) to form a 3D structure (Fig. 7c). To simplify the rather intricate structure of complex 5, the L^{3-} ligand and Cd(II) ion can be simplified as 4-connected nodes, the ligand bib can be reduced to a 2-connected node, and the structure of 5 can be represented as a (4,4,4)-connected net with a point symbol of $\{4\cdot 6^4\cdot 10\}_2\{4\cdot 6^4\cdot 8\}_2\{6^2\cdot 8^4\}$. Of particular interest is the most striking feature of complex 5, that is, a pair of identical 3D single nets is interlocked with each other, thus directly leading to the formation of a 2-fold interpenetrated 3D architecture (Fig. 7d).

Coordination modes of H_3L in complexes 1–5

From the structure descriptions, we found that the carboxylate groups of H_3L exhibit a variety of coordination modes. In this paper, there are five kinds of coordination modes of the carboxylate groups (Scheme 2). In complex 1, the H_3L ligand is partially deprotonated, and the carboxyl group coordinates with Zn(II) ions with a $\mu_2\text{-}\eta_0\text{:}\eta_1\text{:}\eta_1\text{:}\eta_1\text{:}\eta_0\text{:}\eta_0$ coordination mode (mode I). In 2–5, H_3L is completely deprotonated and exhibits different coordination modes. The H_3L ligand in complex 2 links six Zn(II) ions with a $\mu_6\text{-}\eta_1\text{:}\eta_2\text{:}\eta_0\text{:}\eta_1\text{:}\eta_1\text{:}\eta_1$ coordination mode (mode II). In 3, H_3L exhibits the coordination mode $\mu_5\text{-}\eta_2\text{:}\eta_2\text{:}\eta_1\text{:}\eta_1\text{:}\eta_1\text{:}\eta_1$ (mode III). In 4, the wholly deprotonated carboxylate groups of the L^{3-} ligand adopt a $\mu_6\text{-}\eta_1\text{:}\eta_1\text{:}\eta_1\text{:}\eta_2\text{:}\eta_2\text{:}\eta_1$ coordination mode (mode IV). In complex 5, the three carboxyl groups of H_3L adopt the $\mu_4\text{-}\eta_1\text{:}\eta_1\text{:}\eta_1\text{:}\eta_0\text{:}\eta_1\text{:}\eta_1$ coordination mode (mode V). Clearly, the diverse coordination modes of carboxylate groups resulted in the structural differences of complexes 1–5.

Effects of the central metals on the structures

The central metals play important roles in the formation of 1–5. The varieties in coordination numbers of the central metals are an important reason for the complex structure

discrepancies. Because the radius of Cd(II) ions is larger than that of Zn(II) ions, the coordination numbers (n) of the Cd(II) ions in 3 ($n = 6, 8$), 4 and 5 ($n = 6$) are larger than those of the Zn(II) ions in 1 and 2 ($n = 5$). As a result, the structural differences between these complexes may be attributed to the differences in coordination numbers of the metal ions. In other words, it is found that suitable metal ions may be a good candidate for construction of novel high-dimensional coordination polymers.

Effects of the bib ligands on the structures

The differences in the structures of complexes 1 and 2, as well as 3, 4 and 5 indicate that the bib ligands have remarkable effects on the formation of the final structures. Complex 2 exhibits a 3D framework, however, when the bib ligands were introduced into the reaction system of 1, a 2D layer structure was obtained. For complexes 3 and 4, both have a 3D non-interpenetrating framework; when the bib ligands were introduced into the reaction system of 5, a 3D 2-fold interpenetrating network is found. It is obvious that the auxiliary ligands also play an important role in the final results.

Power X-ray diffraction analyses and thermal analysis

To confirm the phase purity of the bulk materials, PXRD experiment has been carried out. The PXRD experimental and computer-simulated patterns, shown in the supplementary material (Fig. S1–S5[†]), are in good agreement with the corresponding simulated one, indicating the phase purity of the products.

The thermal stabilities of 1–5 were measured under nitrogen atmosphere from 30 °C to 800 °C, and the TG-DTG curves are shown in Fig. S6–S10[†]. Complex 1 shows a small weight loss of 6.12% (calcd: 6.05%) in the range of 66–153 °C, corresponding to the loss of lattice water molecules. Upon further heating, the framework starts to collapse. The final residue of 13.72% is close to the calculated 13.66% based on ZnO. For 2, the first weight loss of 11.49% was observed from 35 to 184 °C, corresponding to the loss of water molecules (calcd: 11.14%). Then the skeleton of 2 begins to collapse till the 32.85% residue corresponding to ZnO (calcd: 33.57%) is observed. The TG curve of 3 exhibits two well-separated weight loss stages; the first weight loss is 9.43% in the temperature range of 52–197 °C, which agrees with the loss of the water molecules (calcd: 9.06%), while the second process starts from 309 to 479 °C, which is equivalent to the loss of the L^{3-} ligand. The remaining weight is 38.17%, in accordance with the CdO (calcd: 38.76%). Complex 4 exhibits a weight loss of 9.89% (calcd: 9.77%) in the range of 47–329 °C, corresponding to the loss of acetonitrile and lattice water molecules. Upon further heating, 4 decomposed gradually. Complex 5 exhibits a weight loss of 7.41% (calcd: 7.55%) in the range of 42–284 °C, corresponding to the loss of water molecules. The second process starts from 289 to 790 °C, indicating the decomposition of the

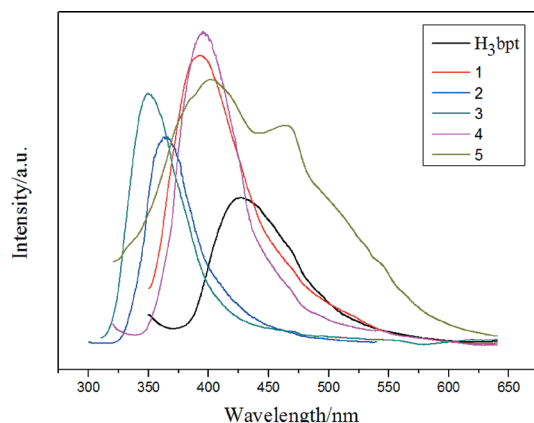


Fig. 8 The solid-state emission spectra of the H₃L ligand and complexes 1–5.

coordination framework; the final residue of 26.63% is close to the calculated 26.90% based on CdO.

Photoluminescence properties

The luminescence properties of complexes containing d¹⁰ metals have been intensely researched owing to their potential applications in photochemistry and sensors.²⁰ Therefore, in this paper, the photoluminescence properties of H₃L, bib and complexes 1–5 were investigated in the solid state at room temperature (Fig. 8). The main emission peaks of H₃L and bib are found at 427 nm ($\lambda_{\text{ex}} = 330$ nm) and 456 nm ($\lambda_{\text{ex}} = 341$ nm),²¹ respectively. The emission bands of these free ligands are probably caused by the $\pi^* \rightarrow \pi$ or $\pi^* \rightarrow n$ transitions.²² Complexes 1–5 display emission peaks at 392, 366, 349, 396 and 401 nm upon excitation at $\lambda = 330, 280, 290, 300$ and 300 nm, respectively. Compared with the emission spectrum of free ligands, blue shifts of emission bands for 1–5 have been observed. Interestingly, for 5, there is another emission peak at 464 nm, which is slightly red-shifted (8 nm) compared with that of the free bib ligand. Since the Zn(II) and Cd(II) ions are difficult to oxidize or to reduce due to their d¹⁰ configuration, the emission of complexes 1–5 is neither metal-to-ligand charge transfer (MLCT) nor ligand-to-metal charge transfer (LMCT) in nature.²³ The emission of the complexes may be assigned to the intraligand fluorescence emission.²⁴

Conclusions

In summary, five coordination polymers based on biphenyl-2,4',5-tricarboxylic acid and bib have been synthesized under solvothermal conditions. Complex 1 shows a 3D supramolecular framework formed by π – π interactions. Complex 2 possesses a 3D framework built upon two Zn(II) ions, one L^{3–} ligand and one μ_3 -OH ion. Complex 3 exhibits a 3D framework with a (3,4,5)-connected $\{4^2 \cdot 6\}_2\{4^2 \cdot 8^4\}\{4^3 \cdot 6 \cdot 8^6\}_2$ topology. Complex 4 features a 3D network with a (4,4,6)-connected $\{4^4 \cdot 6^2\}_3\{4^6 \cdot 6^7 \cdot 8^2\}_2$ topology. Complex 5 displays a 3D 2-fold interpenetrating (4,4,4)-connected framework with a point

symbol of $\{4 \cdot 6^4 \cdot 10\}_2\{4 \cdot 6^4 \cdot 8\}_2\{6^2 \cdot 8^4\}$. It has been proven that biphenyl-2,4',5-tricarboxylic acid is a good candidate for construction of coordination polymers with diverse structures. According to the structures of these five complexes, we have found that the final architecture can be influenced by the coordination mode of the biphenyl-2,4',5-tricarboxylic acid, the central metals and the auxiliary N-donor ligands. The photoluminescence emission shows that these complexes may be good candidates for optical materials.

Acknowledgements

This work was supported by the Agricultural Research Program of Shaanxi province (no. 2013k01-43).

Notes and references

- (a) J. J. Zhang, L. Wojtas, R. W. Larsen, M. Eddaoudi and M. J. Zaworotko, *J. Am. Chem. Soc.*, 2009, **131**, 17040; (b) L. Bastin, P. S. B rcia, E. J. Hurtado, J. A. C. Silva, A. E. Rodrigues and B. Chen, *J. Phys. Chem. C*, 2008, **112**, 1575; (c) D. S. Li, Y. P. Wu, P. Zhang, M. Du, J. Zhao, C. P. Li and Y. Y. Wang, *Cryst. Growth Des.*, 2010, **10**, 2037; (d) S. Kitagawa, R. Kitaura and S. Noro, *Angew. Chem., Int. Ed.*, 2004, **43**, 2334; (e) S. Leininger, B. Olenyuk and P. J. Stang, *Chem. Rev.*, 2000, **100**, 853; (f) D. S. Li, Y. P. Wu, J. Zhao, J. Zhang and J. Y. Lu, *Coord. Chem. Rev.*, 2014, **261**, 1; (g) D. S. Li, X. J. Ke, J. Zhao, M. Du, K. Zou, Q. F. He and C. Li, *CrystEngComm*, 2011, **13**, 3355.
- (a) Y. J. Cui, Y. F. Yue, G. D. Qian and B. L. Chen, *Chem. Rev.*, 2012, **112**, 1126; (b) J. Heine and K. M ller-Buschbaum, *Chem. Soc. Rev.*, 2013, **42**, 9232; (c) M. D. Allendorf, C. A. Bauer, R. K. Bhakta and R. J. T. Houk, *Chem. Soc. Rev.*, 2009, **38**, 1330; (d) N. B. Shustova, A. F. Cozzolino and M. Dinc , *J. Am. Chem. Soc.*, 2012, **134**, 19596; (e) X. H. Chang, Y. Zhao, M. L. Han, L. F. Ma and L. Y. Wang, *CrystEngComm*, 2014, **16**, 6417; (f) L. Zhou, J. Zhang, Y. L. Li and H. B. Du, *CrystEngComm*, 2013, **15**, 8989.
- (a) F. Nouar, J. Eckert, J. F. Eubank, P. Forster and M. Eddaoudi, *J. Am. Chem. Soc.*, 2009, **131**, 2864; (b) A. Aijaz, P. Lama and P. K. Bharadwaj, *Inorg. Chem.*, 2010, **49**, 5883; (c) L. W. Mi, H. W. Hou, Z. Y. Song, H. Y. Han, H. Xu, Y. T. Fan and S. W. Ng, *Cryst. Growth Des.*, 2007, **7**, 2553; (d) B. Manna, A. K. Chaudhari, B. Joarder, A. Karmakar and S. K. Ghosh, *Angew. Chem., Int. Ed.*, 2013, **52**, 998.
- (a) H. H. Wu, Q. H. Gong, D. H. Olson and J. Li, *Chem. Rev.*, 2012, **112**, 836; (b) M. Zhang, Z. J. Pu, X. L. Chen, X. L. Gong, A. X. Zhu and L. M. Yuan, *Chem. Commun.*, 2013, **49**, 5201; (c) T. Borjigin, F. X. Sun, J. L. Zhang, K. Cai, H. Ren and G. S. Zhu, *Chem. Commun.*, 2012, **48**, 7613; (d) I. A. Ibarra, T. W. Hesterberg, B. J. Holliday, V. M. Lynch and S. M. Humphrey, *Dalton Trans.*, 2012, **41**, 8003.
- (a) M. Yoon, R. Srirambalaji and K. Kim, *Chem. Rev.*, 2012, **112**, 1196; (b) B. Gole, A. K. Bar, A. Mallick, R. Banerjee and P. S. Mukherjee, *Chem. Commun.*, 2013, **49**, 7439.

- 6 (a) M. Kurmoo, *Chem. Soc. Rev.*, 2009, 38, 1353; (b) B. K. Tripuramallu, P. Manna, S. N. Reddy and S. K. Das, *Cryst. Growth Des.*, 2012, 12, 777; (c) Q. X. Yang, L. F. Huang, M. D. Zhang, Y. Z. Li, H. G. Zheng and Q. Y. Lu, *Cryst. Growth Des.*, 2013, 13, 440; (d) C. W. Ingram, L. Liao, J. Bacsá, I. Harruna, D. Sabo and Z. J. Zhang, *Cryst. Growth Des.*, 2013, 13, 1131; (e) A. R. Geisheimer, W. Huang, V. Pacradouni, S. A. Sabok-Sayr, J. E. Sonier and D. B. Leznoff, *Dalton Trans.*, 2011, 40, 7505; (f) D. S. Li, F. Fu, J. Zhao, Y. P. Wu, M. Du, K. Zou, W. W. Dong and Y. Y. Wang, *Dalton Trans.*, 2010, 39, 11522.
- 7 (a) H. L. Jiang, B. Liu and Q. Xu, *Cryst. Growth Des.*, 2010, 10, 806; (b) Y. Yang, J. Yang, P. Du, Y. Y. Liu and J. F. Ma, *CrystEngComm*, 2014, 16, 1136; (c) B. Zheng, J. H. Luo, F. Wang, Y. Peng, G. H. Li, Q. S. Huo and Y. L. Liu, *Cryst. Growth Des.*, 2013, 13, 1033.
- 8 (a) M. L. Han, X. H. Chang, X. Feng, L. F. Ma and L. Y. Wang, *CrystEngComm*, 2014, 16, 1687; (b) N. W. Ockwig, O. Delgado-Friedrichs, M. O'Keeffe and O. M. Yaghi, *Acc. Chem. Res.*, 2005, 38, 176; (c) H. L. Wang, D. P. Zhang, D. F. Sun, Y. T. Chen, L. F. Zhang, L. J. Tian, J. Z. Jiang and Z. H. Ni, *Cryst. Growth Des.*, 2009, 9, 5273; (d) H. Y. Bai, J. F. Ma, J. Yang, Y. Y. Liu, H. Wu and J. C. Ma, *Cryst. Growth Des.*, 2010, 10, 995.
- 9 (a) C. L. Zhang, H. Hao, Z. Z. Shi and H. G. Zheng, *CrystEngComm*, 2014, 16, 5662; (b) M. B. Duriska, S. M. Neville and S. R. Batten, *Chem. Commun.*, 2009, 5579; (c) M. M. Dong, L. L. He, Y. J. Fan, S. Q. Zang, H. W. Hou and T. C. W. Mak, *Cryst. Growth Des.*, 2013, 13, 3353.
- 10 (a) D. C. Zhong, W. G. Lu and J. H. Deng, *CrystEngComm*, 2014, 16, 4633; (b) F. Yu, X. J. Kong, Y. Y. Zheng, Y. P. Ren, L. S. Long, R. B. Huang and L. S. Zheng, *Dalton Trans.*, 2009, 9503; (c) D. S. Li, J. Zhao, Y. P. Wu, B. Liu, L. Bai, K. Zou and M. Du, *Inorg. Chem.*, 2013, 52, 8091.
- 11 (a) Z. Q. Shi, Y. Z. Li, Z. J. Guo and H. G. Zheng, *Cryst. Growth Des.*, 2013, 13, 3078; (b) X. Y. Lu, J. W. Ye, Y. Sun, R. F. Bogale, L. M. Zhao, P. Tian and G. L. Ning, *Dalton Trans.*, 2014, 43, 10104.
- 12 (a) J. L. Du, T. L. Hu, J. R. Li, S. M. Zhang and X. H. Bu, *Eur. J. Inorg. Chem.*, 2008, 1059; (b) A. K. Cheetham, C. N. R. Rao and R. K. Feller, *Chem. Commun.*, 2006, 4780; (c) X. Q. Liang, F. Zhang, W. Feng, X. Q. Zou, C. J. Zhao, H. Na, C. Liu, F. X. Sun and G. S. Zhu, *Chem. Sci.*, 2013, 4, 983; (d) B. L. Chen, L. B. Wang, Y. Q. Xiao, F. R. Fronczek, M. Xue, Y. J. Cui and G. D. Qian, *Angew. Chem., Int. Ed.*, 2009, 48, 500; (e) T. Li, X. Liu, Z. P. Huang, Q. Lin, C. L. Lin, Q. G. Zhan, X. D. Xu and Y. P. Cai, *Inorg. Chem. Commun.*, 2014, 39, 70.
- 13 (a) F. Dai, J. Dou, H. He, X. Zhao and D. Sun, *Inorg. Chem.*, 2010, 49, 4117; (b) C. Ren, P. Liu, Y. Y. Wang, W. H. Huang and Q. Z. Shi, *Eur. J. Inorg. Chem.*, 2010, 5545; (c) W. Q. Kan, Y. Y. Liu, J. Yang, Y. Y. Liu and J. F. Ma, *CrystEngComm*, 2011, 13, 4256; (d) S. N. Zhao, S. Q. Su, X. Z. Song, M. Zhu, Z. M. Hao, X. Meng, S. Y. Song and H. J. Zhang, *Cryst. Growth Des.*, 2013, 13, 2756.
- 14 (a) Y. Go, X. Q. Wang, E. V. Anokhina and A. J. Jacobson, *Inorg. Chem.*, 2004, 43, 5360; (b) C. S. Hong and Y. S. You, *Polyhedron*, 2004, 23, 1379; (c) M. Kurmoo, H. Kumagai, M. Akita-Tanaka, K. Inoue and S. Takagi, *Inorg. Chem.*, 2006, 45, 1627; (d) W. J. Shi, L. Hou, D. Li and Y. G. Yin, *Inorg. Chim. Acta*, 2007, 360, 588.
- 15 (a) X. J. Zhao, G. S. Zhu, Q. R. Fang, Y. Wang, F. X. Sun and S. L. Qiu, *Cryst. Growth Des.*, 2009, 9, 737; (b) H. L. Jiang, N. Tsumori and Q. Xu, *Inorg. Chem.*, 2010, 49, 10001; (c) L. H. Xie, Y. Wang, X. M. Liu, J. B. Lin, J. P. Zhang and X. M. Chen, *CrystEngComm*, 2011, 13, 5849.
- 16 (a) Q. Huang, L. H. Diao, C. Zhang and F. H. Lei, *Inorg. Chem. Commun.*, 2011, 14, 1889; (b) J. L. Wang, K. L. Hou, Y. H. Xing, Z. Y. Deng and Z. Shi, *J. Coord. Chem.*, 2011, 64, 3767; (c) R. Cao, D. F. Sun, Y. C. Liang, M. C. Hong, K. Tatsumi and Q. Shi, *Inorg. Chem.*, 2002, 41, 2087; (d) Y. G. Li, N. Hao, E. B. Wang, Y. Lu, C. W. Hu and L. Xu, *Eur. J. Inorg. Chem.*, 2003, 2567.
- 17 (a) X. D. Du, H. P. Xiao, X. H. Zhou, T. Wu and X. Z. You, *J. Solid State Chem.*, 2010, 183, 1464; (b) P. K. Chen, Y. Qi, Y. X. Che and J. M. Zheng, *CrystEngComm*, 2010, 12, 720; (c) D. Sun, L. L. Han, S. Yuan, Y. K. Deng, M. Z. Xu and D. F. Sun, *Cryst. Growth Des.*, 2013, 13, 377.
- 18 (a) X. H. Chang, J. H. Qin, L. F. Ma, J. G. Wang and L. Y. Wang, *Cryst. Growth Des.*, 2012, 12, 4649; (b) T. Liu, S. Wang, J. Lu, J. M. Dou, M. J. Niu, D. C. Li and J. F. Bai, *CrystEngComm*, 2013, 15, 5476; (c) S. J. Wang, Y. W. Tian, L. X. You, F. Ding, K. W. Meert, D. Poelman, P. F. Smet, B. Y. Ren and Y. G. Sun, *Dalton Trans.*, 2014, 43, 3462; (d) Y. P. Li, Y. Chai, G. P. Yang, H. H. Miao, L. Cui, Y. Y. Wang and Q. Z. Shi, *Dalton Trans.*, 2014, 43, 10947.
- 19 (a) Y. L. Lu, W. J. Zhao, Y. Liu, B. Liu, X. Feng, J. T. Tan, X. Li and X. W. Yang, *J. Solid State Chem.*, 2012, 192, 144; (b) Z. J. Lin, B. Xu, T. F. Liu, M. N. Cao, J. Lv and R. Cao, *Eur. J. Inorg. Chem.*, 2010, 3842; (c) Z. J. Zhang, L. Wojtas, M. Eddaoudi and M. J. Zaworotko, *J. Am. Chem. Soc.*, 2013, 135, 5982.
- 20 (a) L. E. Kreno, K. Leong, O. K. Farha, M. Allendorf, R. P. Van Duyne and J. T. Hupp, *Chem. Rev.*, 2012, 112, 1105; (b) G. X. Liu, Y. Q. Huang, Q. Chu, T. A. Okamura, W. Y. Sun, H. Liang and N. Ueyama, *Cryst. Growth Des.*, 2008, 8, 3233; (c) J. Tao, X. Yin, Z. B. Wei, R. B. Huang and L. S. Zheng, *Eur. J. Inorg. Chem.*, 2004, 125; (d) J. Chen, A. Neels and K. M. Fromm, *Chem. Commun.*, 2010, 46, 8282.
- 21 Y. W. Li, H. Ma, Y. Q. Chen, K. H. He, Z. X. Li and X. H. Bu, *Cryst. Growth Des.*, 2012, 12, 189.
- 22 (a) Y. Y. Liu, J. Li, J. F. Ma, J. C. Ma and J. Yang, *CrystEngComm*, 2012, 14, 169; (b) W. Chen, J. Y. Wang, C. Chen, Q. Yue, H. M. Yuan, J. S. Chen and S. N. Wang, *Inorg. Chem.*, 2003, 42, 944.
- 23 (a) J. Yang, Q. Yue, G. D. Li, J. J. Cao, G. H. Li and J. S. Chen, *Inorg. Chem.*, 2006, 45, 2857; (b) A. Thirumurugan and S. Natarajan, *Dalton Trans.*, 2004, 2923.
- 24 (a) D. S. Li, P. Zhang, J. Zhao, Z. F. Fang, M. Du, K. Zou and Y. Q. Mu, *Cryst. Growth Des.*, 2012, 12, 1697; (b) L. P. Zhang, J. F. Ma, Y. Y. Pang, J. C. Ma and J. Yang, *CrystEngComm*, 2010, 12, 4433.